

## 1. Introduction to Crystallography [1]

The solid state includes most of the materials that make modern technology possible. It includes the wide varieties of steel that are used in architecture and engineering, the semiconductors and metallic conductors that are used in information technology and power distribution, the ceramics that increasingly are replacing metals, and the synthetic and natural polymers that are used in the textile industry and in the fabrication of many of the common objects of the modern world. The properties of solids stem, of course, from the arrangement and properties of the constituent atoms, and one of the challenges of this chapter is to see how a wide range of bulk properties, including rigidity, electrical conductivity, and optical and magnetic properties stem from the properties of atoms. One crucial aspect of this link is the pattern in which the atoms (and molecules) are stacked together.

A crystal is built up from regularly repeating ‘structural motifs’, which may be atoms, molecules, or groups of atoms, molecules, or ions. A *space lattice* is the pattern formed by points representing the locations of these motifs (Fig. 1). The space lattice is, in effect, an abstract scaffolding for the crystal structure. More formally, a space lattice is a three-dimensional, infinite array of points, each of which is surrounded in an identical way by its neighbors, and which defines the basic structure of the crystal. In some cases there may be a structural motif centered on each lattice point, but that is not necessary. The crystal structure itself is obtained by associating with each lattice point an identical structural motif.

The *unit cell* is an imaginary parallelepiped (parallel-sided figure) that contains one unit of the translationally repeating pattern (Fig. 2). A unit cell can be thought of as the fundamental region from which the entire crystal may be constructed by purely translational displacements (like bricks in a wall). A unit cell is commonly formed by joining neighboring lattice points by straight lines (Fig. 3). Such unit cells are called primitive. It is sometimes more convenient to draw larger *nonprimitive* unit cells that also have lattice points at their centers or on pairs of opposite faces. An infinite number of different unit cells can describe the same lattice, but the one with sides that have the shortest lengths and that are most nearly perpendicular to one another is normally chosen.

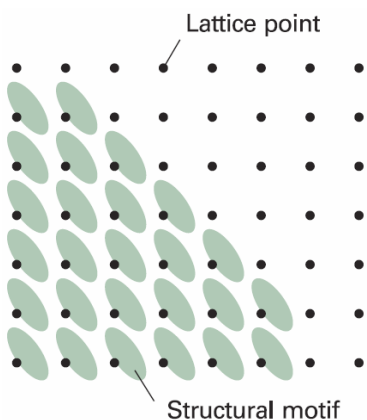


Figure 1. [1]

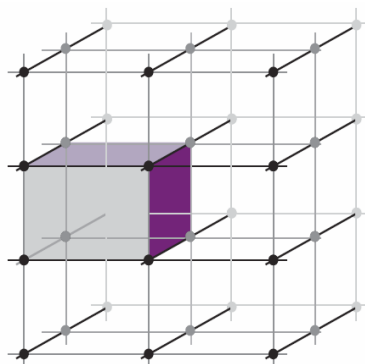


Figure 2. [1]

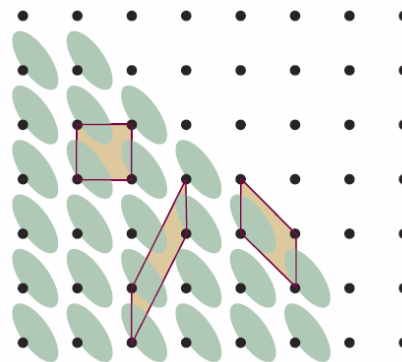


Figure 3. [1]

A unit cell can be represented by a parallelepiped defined by the three basis vectors [2]]. By convention, these are called **a**, **b**, and **c** (Fig. 4). The directions specified by the vectors **a**, **b**, and **c** are the *X*, *Y*, *Z* crystallographic (or simply, *crystal*) axes, respectively. Note that unlike Cartesian axes, crystallographic axes (and, of course, vectors **a**, **b**, and **c**) are not necessarily orthogonal to each other! The angles between vectors **a**, **b**, and **c** are indicated by  $\alpha$ ,  $\beta$ , and  $\gamma$ , with

$\alpha$  opposing **a**,  $\beta$  opposing **b**, and  $\gamma$  opposing **c** (Fig. 4). The volume of the unit cell  $V_c$  is then given by [2]

$$V_c = \mathbf{a} \cdot \mathbf{b} \times \mathbf{c} \quad (1)$$

where the symbol '.' indicates the scalar (dot) product and the symbol '×' - the vector (cross) product. Note that when calculating the scalar (dot) product of two vectors defined in the crystallographic frame, you can *not* apply formula for the Cartesian frame [3]

$$\mathbf{p}^T \mathbf{q} = \mathbf{q}^T \mathbf{p} = \sum_i p_i q_i \quad (2)$$

because the crystallographic axes are not necessarily orthogonal to each other (see Figure 4). One way to calculate the dot product of two vectors **r** and **s** is to define them in the Cartesian frame (see section 6) and then use equation (2). Alternatively, recall that the dot product of two vectors **r** and **s** is given by

$$\mathbf{r} \cdot \mathbf{s} = |\mathbf{r}| |\mathbf{s}| \cos \vartheta \quad (3)$$

where the magnitudes of vectors **r** and **s** are denoted by  $|\mathbf{r}|$  and  $|\mathbf{s}|$ , respectively, and  $\vartheta$  is the angle between **r** and **s**.

The orientation of the three crystallographic axes is usually chosen in such a way that an observer located along the positive direction of **c** sees **a** moving towards **b** by an anti-clockwise rotation. The lengths of vectors **a**, **b**, and **c** are denoted as  $a$ ,  $b$ , and  $c$ , which, when combined with the angles between them ( $\alpha$ ,  $\beta$ , and  $\gamma$ ) are called *the unit cell parameters*. By convention the lengths of the *unit cell axes*  $a$ ,  $b$ , and  $c$  are given in angstroms (Å), and the *unit cell angles* ( $\alpha$ ,  $\beta$ , and  $\gamma$ ) are given in degrees (°).

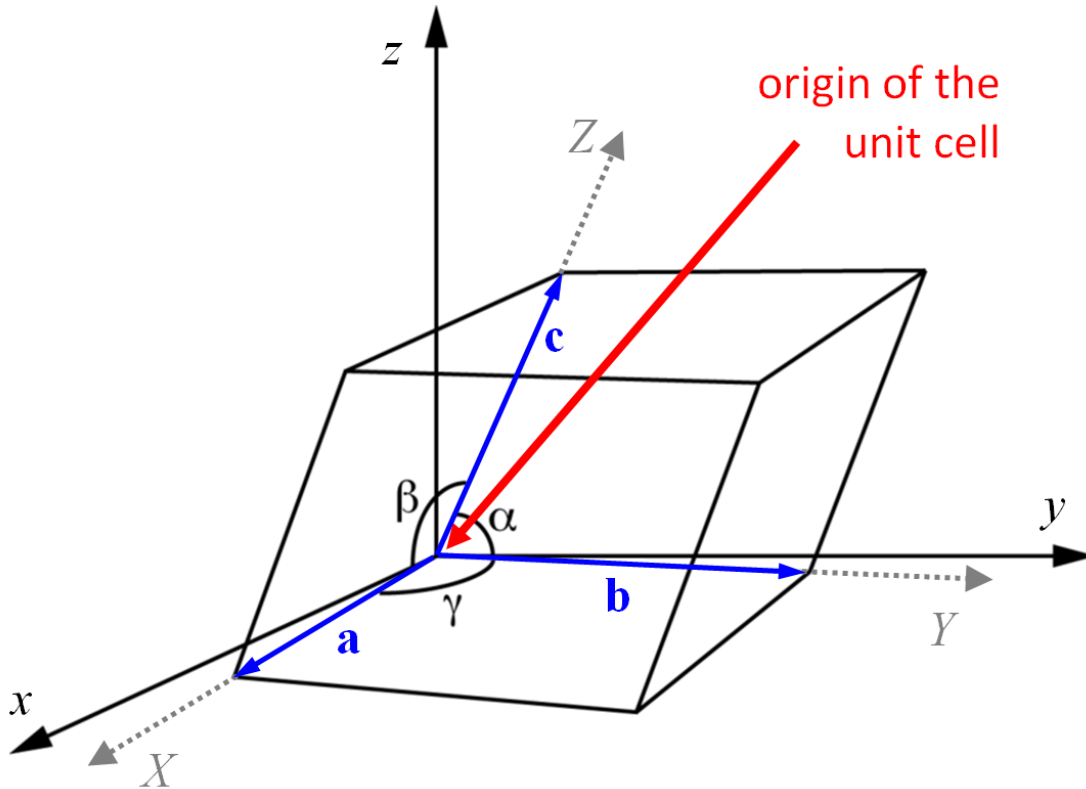


**Figure 4.** Notation for a unit cell. Cartesian axes are denoted as  $x$ ,  $y$ , and  $z$ . Unit cell vectors **a**, **b**, and **c** are defined along the crystallographic (crystal) axes  $X$ ,  $Y$ , and  $Z$  which are not necessarily orthogonal to each other.

Unit cells are classified into seven crystal systems by noting the rotational *symmetry elements* they possess. A *symmetry operation* is an action (such as a rotation, reflection, or inversion) that leaves an object looking the same after it has been carried out. There is a corresponding symmetry element for each symmetry operation, which is the point, line, or plane with respect to which the symmetry operation is performed. For instance, an  $n$ -fold rotation (the symmetry operation) about an  $n$ -fold axis of symmetry (the corresponding symmetry element) is a rotation through  $360^\circ/n$ .

A *cubic* unit cell, for example, has four threefold axes in a tetrahedral array (Fig. 5). A *monoclinic* unit cell has one twofold axis; the unique axis is by convention the  $b$  axis (Fig. 6). A *triclinic* unit cell has no rotational symmetry, and typically all three sides and angles are different (Fig. 7). Table 1 lists the essential symmetries, the elements that must be present for the unit cell to belong to a particular crystal system.

There are only 14 distinct space lattices in three dimensions. These *Bravais lattices* are illustrated in Fig. 8. It is conventional to portray these lattices by primitive unit cells in some cases and by non-primitive unit cells in others. A *primitive unit cell* (with lattice points only at the corners) is denoted P. A *body-centered unit cell* (I) also has a lattice point at its centre. A *face-centered unit cell* (F) has lattice points at its corners and also at the centers of its six faces. A *side-centered unit cell* (A, B, or C) has lattice points at its corners and at the centers of two opposite faces. For simple structures, it is often convenient to choose an atom belonging to the structural motif, or the centre of a molecule, as the location of a lattice point or the vertex of a unit cell, but that is not a necessary requirement.

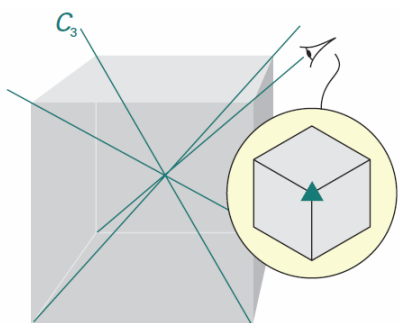


**Figure 5.** A unit cell belonging to the *cubic* system has four threefold axes, arranged tetrahedrally. [1]

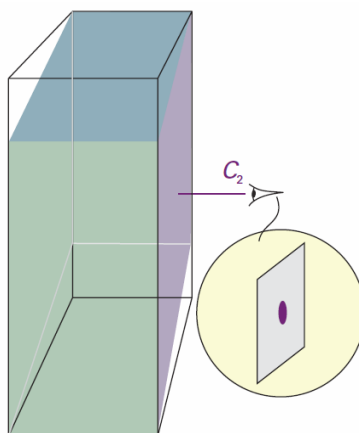


**Figure 6.** A unit cell belonging to the *monoclinic* system has a twofold axis (denoted  $C_2$ ). [1]

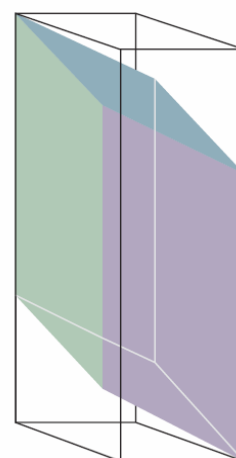


**Figure 7.** A *triclinic* unit cell has no axes of rotational symmetry. [1]

**Table 1.** The seven crystal systems [1]

System	Essential symmetries	Unit Cell Parameters
Triclinic	None	$a, b, c, \alpha, \beta, \gamma$
Monoclinic	One 2-fold axis	$a, b, c, 90, \beta, 90$
Orthorhombic	Three perpendicular 2-fold axes	$a, b, c, 90, 90, 90$
Rhombohedral (Trigonal)	One 3-fold axis	$a, a, c, 90, 90, 90$
Tetragonal	One 4-fold axis	$a, a, c, 90, 90, 120$
Hexagonal	One 6-fold axis	$a, a, c, 90, 90, 120$
Cubic	Four 3-fold axes in a tetrahedral arrangement	$a, a, a, 90, 90, 90$

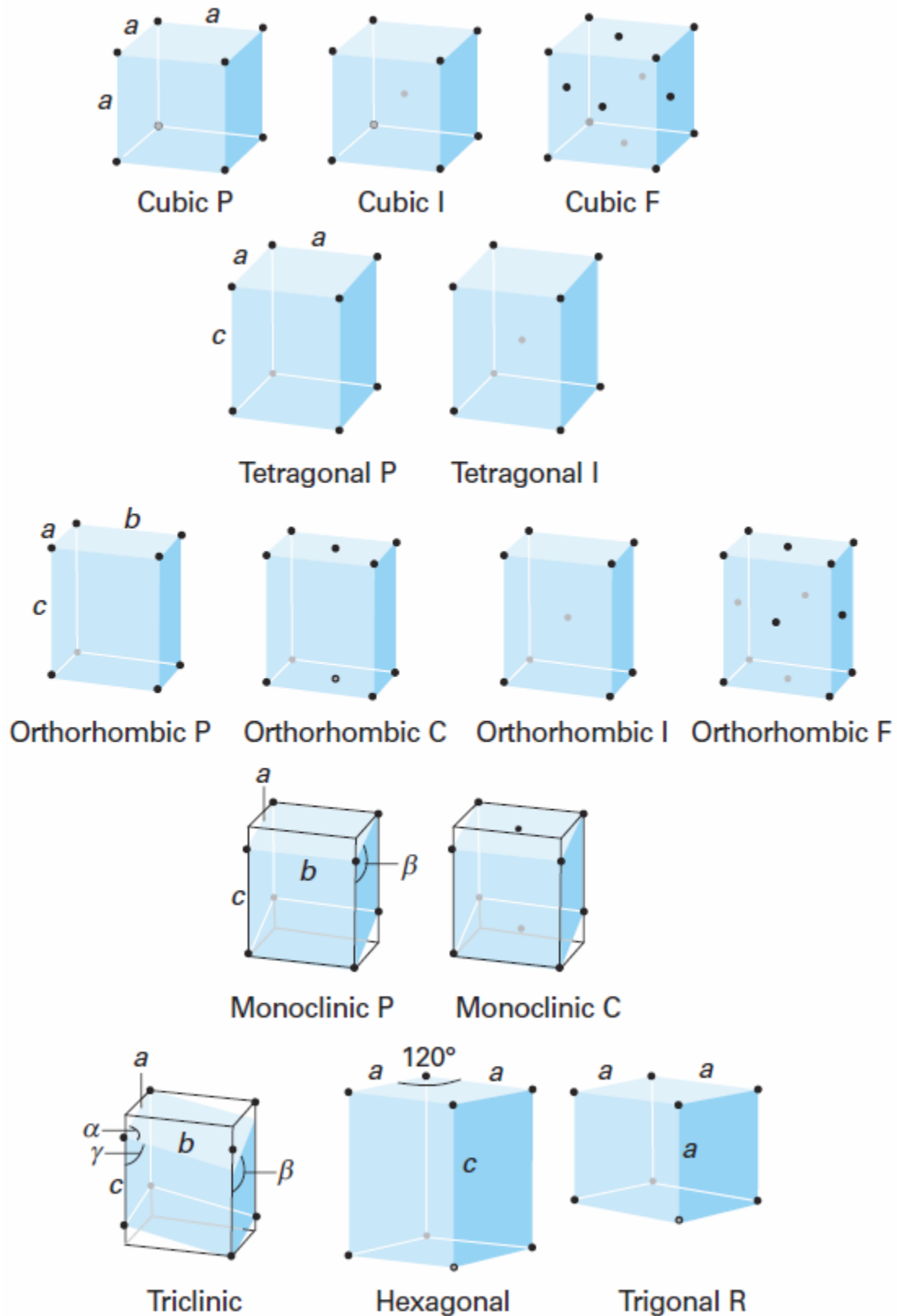


**Figure 8.** The fourteen Bravais lattices. The points are lattice points, and are not necessarily occupied by atoms. P denotes a primitive unit cell (R is used for a trigonal lattice), I a bodycentred unit cell, F a face-centred unit cell, and C (or A or B) a cell with lattice points on two opposite faces. [1]

## 2. Introduction to X-ray Crystallography [1]

A characteristic property of waves is that they interfere with one another, giving a greater displacement where peaks or troughs coincide and a smaller displacement where peaks coincide with troughs (Fig. 9). According to classical electromagnetic theory, the intensity of electromagnetic radiation is proportional to the square of the amplitude of the waves. Therefore, the regions of constructive or destructive interference show up as regions of enhanced or diminished intensities. The phenomenon of *diffraction* is the interference caused by an object in the path of waves, and the pattern of varying intensity that results is called *the diffraction pattern*. Diffraction occurs when the dimensions of the diffracting object are comparable to the wavelength of the radiation.

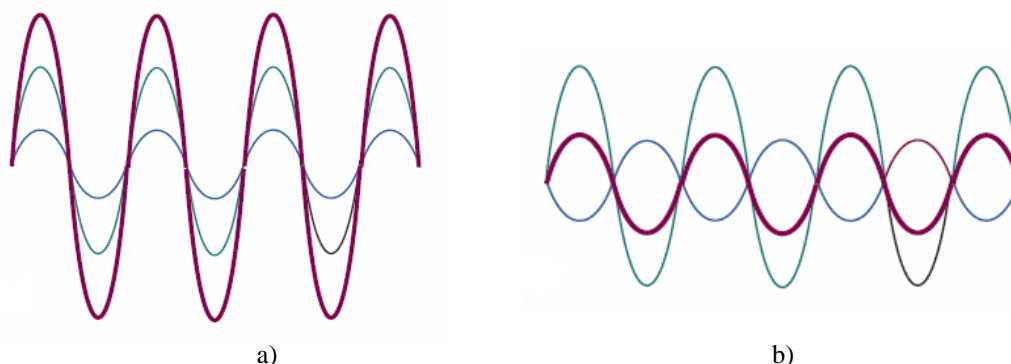


**Figure 9.** When two waves are in the same region of space they interfere. Depending on their relative phase, they may interfere (a) constructively, to give an enhanced amplitude, or (b) destructively, to give a smaller amplitude. The component waves are shown in green and blue and the resultant in purple. [1]

X-rays are electromagnetic radiation with wavelengths of the order of  $10^{-10}$  m ( $\text{\AA}$ ). They are typically generated by bombarding a metal with high-energy electrons. The electrons decelerate as they plunge into the metal and generate radiation with a continuous range of wavelengths called *Bremsstrahlung*. Superimposed on the continuum are a few high-intensity, sharp peaks (Fig. 10). These peaks arise from collisions of the incoming electrons with the electrons in the inner shells of the atoms. A collision expels an electron from an inner shell, and an electron of higher energy drops into the vacancy, emitting the excess energy as an X-ray photon (Fig. 11). If the electron falls into a *K* shell (a shell with principal quantum number  $n = 1$ ), the X-rays are classified as *K*-radiation, and similarly for transitions into the *L* ( $n = 2$ ) and *M* ( $n = 3$ ) shells. Transitions with  $\Delta n = 1$  are called  $\alpha$ , while transitions with  $\Delta n = 2$  are called  $\beta$  etc. Strong, distinct lines are labeled  $K\alpha$ ,  $K\beta$ , and so on. In many-electron atoms energies of electronic subshells of a given shell are not the same, transitions from the same shell ( $n$ ) but different subshells ( $l = 0, \dots, n-1$ ) will result in energy splitting of transitions ( $\alpha_1, \alpha_2, \beta_1, \beta_2, \dots$  etc.). Table 2 shows X-ray *K*-series spectral line wavelengths for some common target materials. Increasingly, X-ray diffraction makes use of the radiation available from synchrotron sources, for its high intensity greatly enhances the sensitivity of the technique.

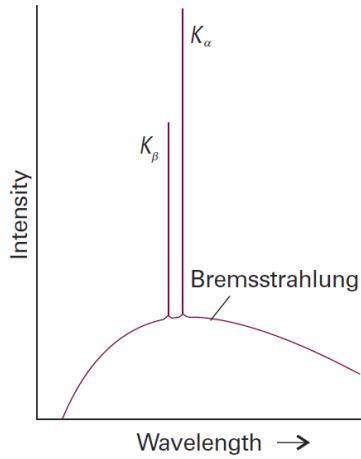


Figure 10. [1]

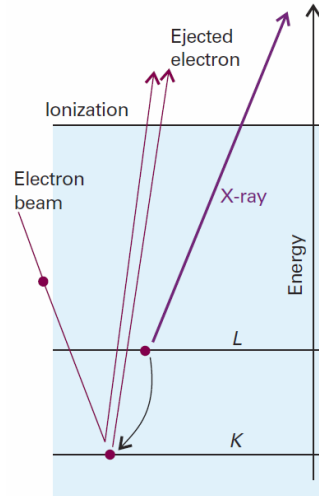


Figure 11. [1]

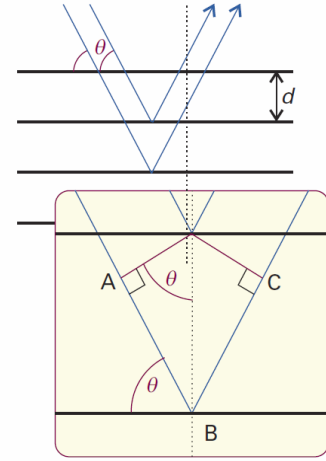


Figure 12. [1]

**Table 2.** X-ray  $K$ -series spectral line wavelengths ( $\text{\AA}$ ) for some common target materials

Target	$K_{\beta_1}$	$K_{\beta_2}$	$K_{\alpha_1}$	$K_{\alpha_2}$
Fe	1.7566	1.7442	1.93604	1.93998
Co	1.62079	1.60891	1.78897	1.79285
Ni	1.5001	1.4886	1.65791	1.66175
Cu	1.39222	1.38109	1.54056	1.54439
Zr	0.70173	0.68993	0.78593	0.79015
Mo	0.63229	0.62099	0.70930	0.71359

An early approach to the analysis of diffraction patterns produced by crystals was to regard a lattice plane as a semi-transparent mirror, and to model a crystal as stacks of reflecting lattice planes of separation  $d$  (Fig. 12). The model makes it easy to calculate the angle the crystal must make to the incoming beam of X-rays for constructive interference to occur. It has also given rise to the name reflection to denote an intense beam arising from constructive interference.

Consider the reflection of two parallel rays of the same wavelength by two adjacent planes of a lattice, as shown in Fig. 12. One ray strikes point D on the upper plane but the other ray must travel an additional distance AB before striking the plane immediately below. Similarly, the reflected rays will differ in path length by a distance BC. The net path length difference of the two rays is then

$$AB + BC = 2d \sin \theta \quad (4)$$

where  $\theta$  is the *glancing angle*. For many glancing angles the path-length difference is not an integer number of wavelengths, and the waves interfere largely destructively. However, when the path-length difference is an integer number of wavelengths ( $AB + BC = n\lambda$ ), the reflected waves are in phase and interfere constructively. It follows that a reflection should be observed when the glancing angle satisfies Bragg's law:

$$n\lambda = 2d \sin \theta \quad (5)$$

Reflections with  $n = 2, 3, \dots$  are called second-order, third-order, and so on; they correspond to path-length differences of 2, 3, ... wavelengths. In modern work it is normal to absorb the  $n$  into  $d$ , to write the Bragg law as

$$\lambda = 2d \sin \theta \quad (6)$$

and to regard the  $n$ th-order reflection as arising from the  $\{nh, nk, nl\}$  planes.

The primary use of Bragg's law is in the determination of the spacing between the layers in the lattice for, once the angle  $\theta$  corresponding to a reflection has been determined,  $d$  may readily be calculated.

### 3. Introduction to Fourier series and Fourier transforms [4]

A continuous, single-valued, periodic function  $f(x)$  has a Fourier transform defined by

$$g(n) = \int_{-\infty}^{+\infty} f(x) e^{2\pi i n x} dx \quad (7)$$

and the inverse (back-) transform is

$$f(x) = \int_{-\infty}^{+\infty} g(n) e^{-2\pi i n x} dn \quad (8)$$

According to *Fourier's theorem*, any continuous, differentiable, single-valued, and periodic function  $f(x)$  with a period of  $2\pi$  can be expanded in terms of sine and cosine series as

$$f(x) = a(0) + \sum_{n=1}^{\infty} \{a(n) \cos(nx) + b(n) \sin(nx)\} \quad (9)$$

where  $a(n)$  and  $b(n)$  are appropriately chosen coefficients. Introducing the following notation,

$$A(n) = \frac{a(n)}{2}, \quad A(-n) = \frac{a(n)}{2}, \quad B(n) = \frac{b(n)}{2}, \quad B(-n) = -\frac{b(n)}{2}, \quad A(0) = a(0) \quad (10)$$

each term in series (9) [except the one with  $n=0$ ] can be represented by

$$A(n) \cos nx + A(-n) \cos(-nx) + B(n) \sin nx + B(-n) \sin(-nx) \quad (11)$$

so series (9) can be written as

$$f(x) = \sum_{n=-\infty}^{\infty} \{A(n) \cos(nx) + B(n) \sin(nx)\} \quad (12)$$

or

$$f(x) = A(0) + \sum_{n=1}^{\infty} \{2A(n) \cos(nx) + 2B(n) \sin(nx)\} \quad (13)$$

Suppose, the period of function  $f(x)$  is not equal to  $2\pi$ , but is some arbitrary value  $a$  (Figure 13).

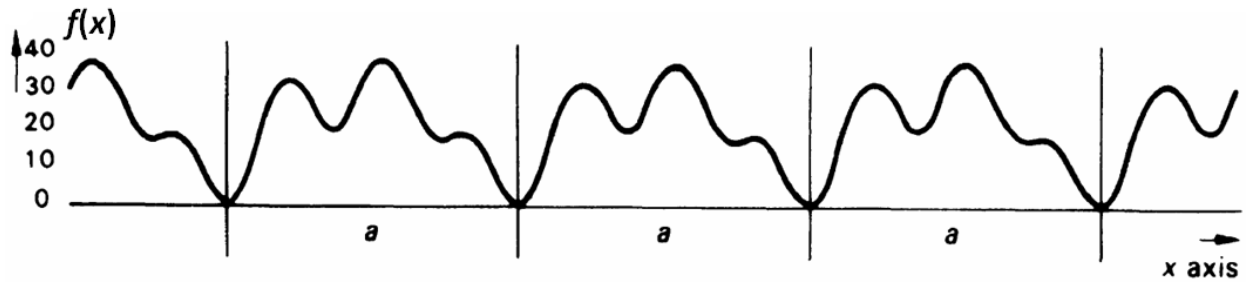


Figure 13. One-dimensional periodic function  $f(x)$  of period  $a$ . [5]

Introducing the new argument  $2\pi x/a$ , the general Fourier series can be written as

$$f(x) = \sum_{n=-\infty}^{\infty} \left\{ A(n) \cos\left(2\pi n \frac{x}{a}\right) + B(n) \sin\left(2\pi n \frac{x}{a}\right) \right\} \quad (14)$$



$$f(x) = A(0) + \sum_{n=1}^{\infty} \left\{ 2A(n) \cos\left(2\pi n \frac{x}{a}\right) + 2B(n) \sin\left(2\pi n \frac{x}{a}\right) \right\} \quad (15)$$

The coefficients of the Fourier series are given by

$$A(0) = \frac{1}{a} \int_0^a f(x) dx \quad (16)$$

$$A(n) = \frac{1}{a} \int_0^a f(x) \cos\left(2\pi n \frac{x}{a}\right) dx \quad (17)$$

$$B(n) = \frac{1}{a} \int_0^a f(x) \sin\left(2\pi n \frac{x}{a}\right) dx \quad (18)$$

A slightly different formula for the series can be obtained by introducing new coefficients:

$$C(n) = \sqrt{A(n)^2 + B(n)^2} \quad (19)$$

$$\tan \phi(n) = \frac{B(n)}{A(n)} \quad (20)$$

which gives

$$\begin{aligned} A(n) &= C(n) \cos \phi(n) \\ B(n) &= C(n) \sin \phi(n) \\ A(0) &= C(0) \end{aligned} \quad (21)$$

and

$$f(x) = \sum_{n=-\infty}^{\infty} \left\{ C(n) \cos\left(2\pi n \frac{x}{a} - \phi(n)\right) \right\} \quad (22)$$

Finally, using the *de Moivre's / Euler's theorem*

$$e^{\pm i\phi} = \cos \phi \pm i \sin \phi \quad (23)$$

and defining

$$\begin{aligned} K(n) &= C(n) e^{i\phi(n)} = A(n) + iB(n) \\ K(-n) &= C(n) e^{-i\phi(n)} = A(n) - iB(n) \end{aligned} \quad (24)$$

we get

$$f(x) = \sum_{n=-\infty}^{\infty} K(n) e^{-i2\pi n \frac{x}{a}} \quad (25)$$

$$K(n) = \frac{1}{a} \int_0^a f(x) e^{i2\pi n \frac{x}{a}} dx \quad (26)$$

Note that

$$K(-n) = K(n)^* \quad (27)$$

i.e. coefficient  $K(-n)$  is a complex-conjugate of coefficient  $K(n)$ .

The summations of a Fourier series extend, theoretically, from  $-\infty$  to  $\infty$  [6]. In practice, however, the range becomes  $n_{\min} \leq n \leq n_{\max}$ , where the limits of  $n$  are preset, normally by experimental conditions. It is notable that increasing  $n_{\max}$  has a dramatic effect on the series. As  $n_{\max}$  increases the series approaches more closely the function  $f(x)$ . In general, the more independent terms that can be included in a Fourier series, the better it represents the periodic function under investigation, from which the terms have been derived.

The process of determining the coefficients of a *Fourier series* is called *Fourier analysis*, and the process of reconstructing the function by the summation of a series is called *Fourier synthesis* [5].

For a function of several variables  $f(xyz)$  with period  $a$  along the  $x$ -axis,  $b$  along the  $y$ -axis, and  $c$  along the  $z$ -axis [4]:

$$f(xyz) = \sum_{h=-\infty}^{\infty} \sum_{k=-\infty}^{\infty} \sum_{l=-\infty}^{\infty} K(hkl) e^{-i2\pi \left( h \frac{x}{a} + k \frac{y}{b} + l \frac{z}{c} \right)} \quad (28)$$

$$K(hkl) = \frac{1}{abc} \int_{x=0}^a \int_{y=0}^b \int_{z=0}^c f(xyz) e^{i2\pi \left( h \frac{x}{a} + k \frac{y}{b} + l \frac{z}{c} \right)} dz dy dx \quad (29)$$

$$K(\bar{h}\bar{k}\bar{l}) = K(hkl)^* \quad (30)$$

where notation  $(\bar{h}\bar{k}\bar{l})$  means  $(-h, -k, -l)$ . Introducing the same kind of coefficients as in the case for the function of a single variable,

$$K(hkl) = C(hkl)e^{i\phi(hkl)} = A(hkl) + iB(hkl) \quad (31)$$

$$K(\bar{h}\bar{k}\bar{l}) = C(hkl)e^{-i\phi(hkl)} = A(hkl) - iB(hkl)$$

we get:

$$f(xyz) = \sum_{h=-\infty}^{\infty} \sum_{k=-\infty}^{\infty} \sum_{l=-\infty}^{\infty} \left\{ \begin{aligned} &A(hkl) \cos \left[ 2\pi \left( h \frac{x}{a} + k \frac{y}{b} + l \frac{z}{c} \right) \right] \\ &+ B(hkl) \sin \left[ 2\pi \left( h \frac{x}{a} + k \frac{y}{b} + l \frac{z}{c} \right) \right] \end{aligned} \right\} \quad (32)$$

$$f(xyz) = \sum_{h=-\infty}^{\infty} \sum_{k=-\infty}^{\infty} \sum_{l=-\infty}^{\infty} \left\{ C(hkl) \cos \left[ 2\pi \left( h \frac{x}{a} + k \frac{y}{b} + l \frac{z}{c} \right) \right] - \phi(hkl) \right\} \quad (33)$$

where

$$A(hkl) = \frac{1}{abc} \int_{x=0}^a \int_{y=0}^b \int_{z=0}^c f(xyz) \cos \left[ 2\pi \left( h \frac{x}{a} + k \frac{y}{b} + l \frac{z}{c} \right) \right] dz dy dx \quad (34)$$

$$B(hkl) = \frac{1}{abc} \int_{x=0}^a \int_{y=0}^b \int_{z=0}^c f(xyz) \sin \left[ 2\pi \left( h \frac{x}{a} + k \frac{y}{b} + l \frac{z}{c} \right) \right] dz dy dx \quad (35)$$

From these formulas it follows that

$$\begin{aligned} A(\bar{h}\bar{k}\bar{l}) &= A(hkl) & B(\bar{h}\bar{k}\bar{l}) &= -B(hkl) \\ C(\bar{h}\bar{k}\bar{l}) &= C(hkl) & \phi(\bar{h}\bar{k}\bar{l}) &= -\phi(hkl) \end{aligned} \quad (36)$$

Therefore, it is possible to reduce the limit of summation over one index (whichever is more convenient) by a factor of two. For example,

$$f(xyz) = A(000) + 2 \sum_{h=1}^{\infty} \sum_{k=-\infty}^{\infty} \sum_{l=-\infty}^{\infty} \left\{ \begin{aligned} &A(hkl) \cos \left[ 2\pi \left( h \frac{x}{a} + k \frac{y}{b} + l \frac{z}{c} \right) \right] \\ &+ B(hkl) \sin \left[ 2\pi \left( h \frac{x}{a} + k \frac{y}{b} + l \frac{z}{c} \right) \right] \end{aligned} \right\} \quad (37)$$

#### 4. Fourier series in X-ray Crystallography [5]

X-rays are scattered by the electrons associated with atoms in a crystal. The scattering of is caused by the oscillations an incoming electromagnetic wave generates in the electrons of atoms, and heavy atoms give rise to stronger scattering than light atoms. The concentration of electrons and its distribution around an atom is called the electron density, and it is measured in electrons per unit volume (usually  $\text{\AA}^{-3}$  or  $\text{nm}^{-3}$ ). At any point  $(x,y,z)$  the electron density is written normally as  $\rho(xyz)$ , and we may identify  $\rho(xyz)$  with the function  $f(xyz)$  discussed in the previous section, while the function  $K(hkl)$  when applied to scattering of electrons on crystals is called the *generalized structure factor*,  $F(hkl)$

In a three-dimensional periodic system (crystal), the *generalized structure factor*  $F(hkl)$  is given by the Fourier transform of the electron density distribution function  $\rho(xyz)$ :

$$F(hkl) = V_c \int_0^1 \int_0^1 \int_0^1 \rho(x_f y_f z_f) e^{i2\pi(hx_f + ky_f + lz_f)} dx_f dy_f dz_f \quad (38)$$

where the integration is over the entire unit cell,  $V_c$  is a volume of the unit cell, and  $\{x_f, y_f, z_f\}$  are the fractional coordinates defined with respect to (w.r.t.) the lengths of unit cell axes  $a$ ,  $b$  and  $c$ :

$$\mathbf{x}_f = \begin{pmatrix} x_f \\ y_f \\ z_f \end{pmatrix} = \begin{pmatrix} x/a \\ y/b \\ z/c \end{pmatrix} \quad (39)$$

Defining [with some simplification] the scattering vector  $\mathbf{S}$  as,

$$\mathbf{S} = \begin{pmatrix} h \\ k \\ l \end{pmatrix} \quad (40)$$

equation (38) can be re-written in the following form

$$F(\mathbf{S}) = V_c \int_0^1 \rho(\mathbf{x}_f) e^{i2\pi(\mathbf{S} \cdot \mathbf{x}_f)} d^3 \mathbf{x}_f \quad (41)$$

where the symbol ' $\cdot$ ' indicates the scalar (dot) product. In general, the *inverse Fourier transform* (also called *back-transform*) of  $F(\mathbf{S})$  should give back  $\rho(\mathbf{x}_f)$

$$\rho(\mathbf{x}_f) = \frac{1}{V_c} \int F(\mathbf{S}) e^{-i2\pi(\mathbf{S} \cdot \mathbf{x}_f)} d^3 \mathbf{S} \quad (42)$$

but because we register  $F(\mathbf{S})$  not in terms of a continuous distribution but as discrete series in  $(hkl)$ , integral (42) is replaced by a summation

$$\rho(\mathbf{x}_f) = \frac{1}{V_c} \sum_{h=h_{\min}}^{h_{\max}} \sum_{k=k_{\min}}^{k_{\max}} \sum_{l=l_{\min}}^{l_{\max}} F(hkl) e^{-i2\pi(hx_f + ky_f + lz_f)} \quad (43)$$

This equation is called a *Fourier synthesis* of the electron density.

Although  $F(hkl)$  has the quality of a vector, it is conventional not to represent it normally in bold (vector) type;  $F(hkl)$  refers to the combined scattering from the electrons in the unit cell to give the  $hkl$ -th spectrum, or the wave from the  $(hkl)$  planes, relative to the scattering by a single electron at the origin.

According to de Moivre's / Euler's theorem, equation (41) can be re-written in terms of cosine (real) and sine (imaginary) components

$$\rho(\mathbf{x}_f) = \frac{1}{V_c} \sum_{h=h_{\min}}^{h_{\max}} \sum_{k=k_{\min}}^{k_{\max}} \sum_{l=l_{\min}}^{l_{\max}} \{A(hkl) \cos[2\pi(hx_f + ky_f + lz_f)] + B(hkl) \sin[2\pi(hx_f + ky_f + lz_f)]\} \quad (44)$$

where

$$A(hkl) = |F(hkl)| \cos \phi(hkl) \quad (45)$$

$$B(hkl) = |F(hkl)| \sin \phi(hkl) \quad (46)$$

The physical meaning of parameters  $A(hkl)$  and  $B(hkl)$  can be readily identified using the so-called *Argand diagram* shown in Figure 14.

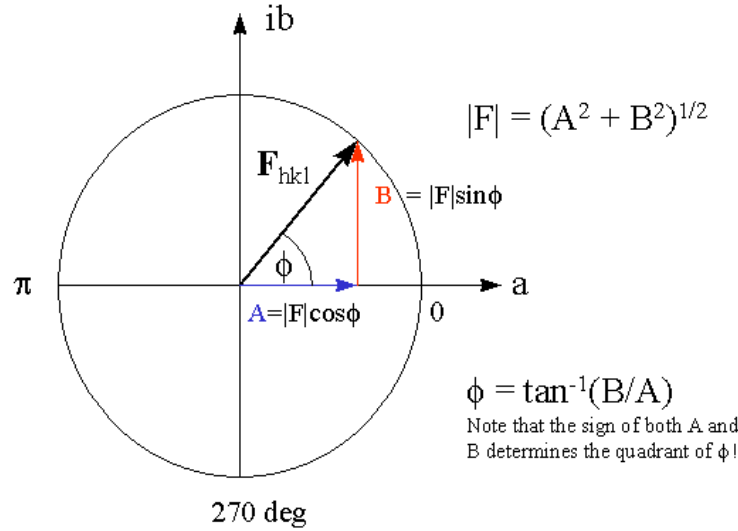


**Figure 14.** The Argand diagram.

Another way of writing a formula for the electron density in terms of structure factors is:

$$\rho(\mathbf{x}_f) = \frac{1}{V_c} \sum_{h=h_{\min}}^{h_{\max}} \sum_{k=k_{\min}}^{k_{\max}} \sum_{l=l_{\min}}^{l_{\max}} |F(hkl)| \cos[2\pi(hx_f + ky_f + lz_f) - \phi(hkl)] \quad (47)$$

where  $\phi(hkl)$  is the *phase angle* (or simply *phase*) of the reflection  $hkl$ . This shows how the electron density depends upon the phase angles: usually, only  $|F(hkl)|$  is measured by experiment,  $\phi(hkl)$  must be determined before equation (47) can be summed. This situation constitutes the *phase problem in crystallography*.

The structure factor of the reflection  $\bar{h}\bar{k}\bar{l}$  is equal to the complex conjugate  $F^*(hkl)$  of  $F(hkl)$  [6]. The structure amplitudes of the reflections  $hkl$  and  $\bar{h}\bar{k}\bar{l}$  are thus equal:

$$|F\bar{h}\bar{k}\bar{l}|^2 = |F(hkl)|^2 \quad (48)$$

This equation represents *Friedel's law*: the intensities of the reflections  $hkl$  and  $\bar{h}\bar{k}\bar{l}$  are equal, even if the crystal is non-centrosymmetric. Thus, except where anomalous scattering is significant, X-ray diffraction spectra form a centrosymmetric array.

### 5. Computational exercise. Objectives.

Suppose, [another] experimental chemist [this time, crystallographer] approaches you and says:

*"Hello Computational Scientist, I have collected an excellent set of X-ray diffraction data for a new crystal. I have done what no one had done before - I was able to measure both the real and imaginary components,  $A(hkl)$  and  $B(hkl)$ , for each reflection  $(hkl)$ . The only problem is, I do not know where the atoms are. Please write a computer program (in Mathematica, Maple, Matlab, Fortran, Pascal, C, C++ etc.) that can automatically read my data files (the format is described below), and use the Newton-Raphson and eigenvector following methods [implemented in the same code with an option to switch between them!] to search for maxima in the electron density distribution constructed via Fourier synthesis. The program should have a user-friendly output, i.e. I would like it to tell me what it does as it is running (remember, you are dealing with a chemist here), and at the very end it should print out a list of peaks and for each peak provide its location in terms of fractional coordinates, and the value of the electron density. Finally, the runtime of the program should be under 1 hour for the collected dataset. It should be easy for you, right?"*

For this exercise your instructor has created a simulated crystal structure of  $(B_3N_3H_9IBrCl)$ . The shape of the molecule is shown in Figure 15.

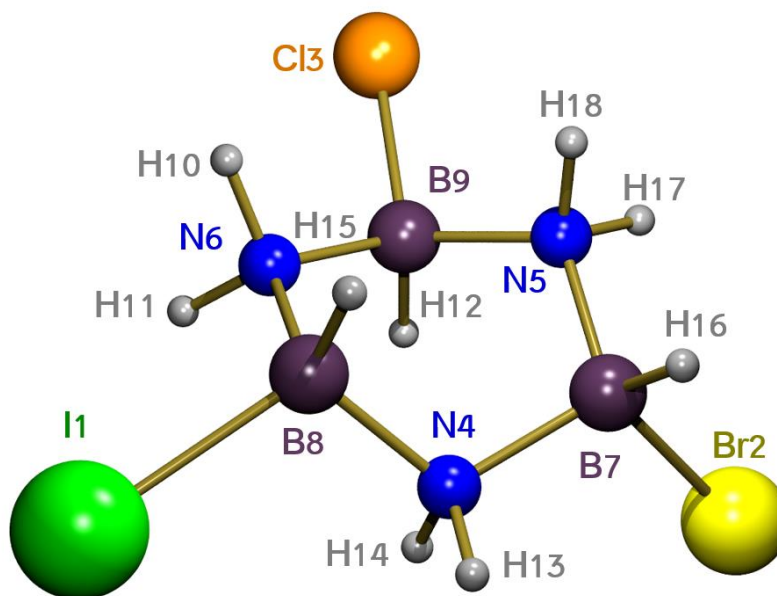


**Figure 15.** The geometry of a  $(B_3N_3H_9IBrCl)$  molecule.

We know the unit cell parameters for the crystal structure of  $(B_3N_3H_9IBrCl)$ , and we have a set of crystal structure factors  $F(hkl)$  with both the real ( $A(hkl)$ ) and imaginary ( $B(hkl)$ ) components determined, but the locations of the  $(B_3N_3H_9IBrCl)$  atoms in the unit cell are not known. The task is to use the Fourier synthesis to generate the electron density  $\rho(xyz)$  and search for peaks that identify the locations of atoms.

The simulated crystal structure includes one  $(B_3N_3H_9IBrCl)$  molecule in the very center of the unit cell (see Figure 16).

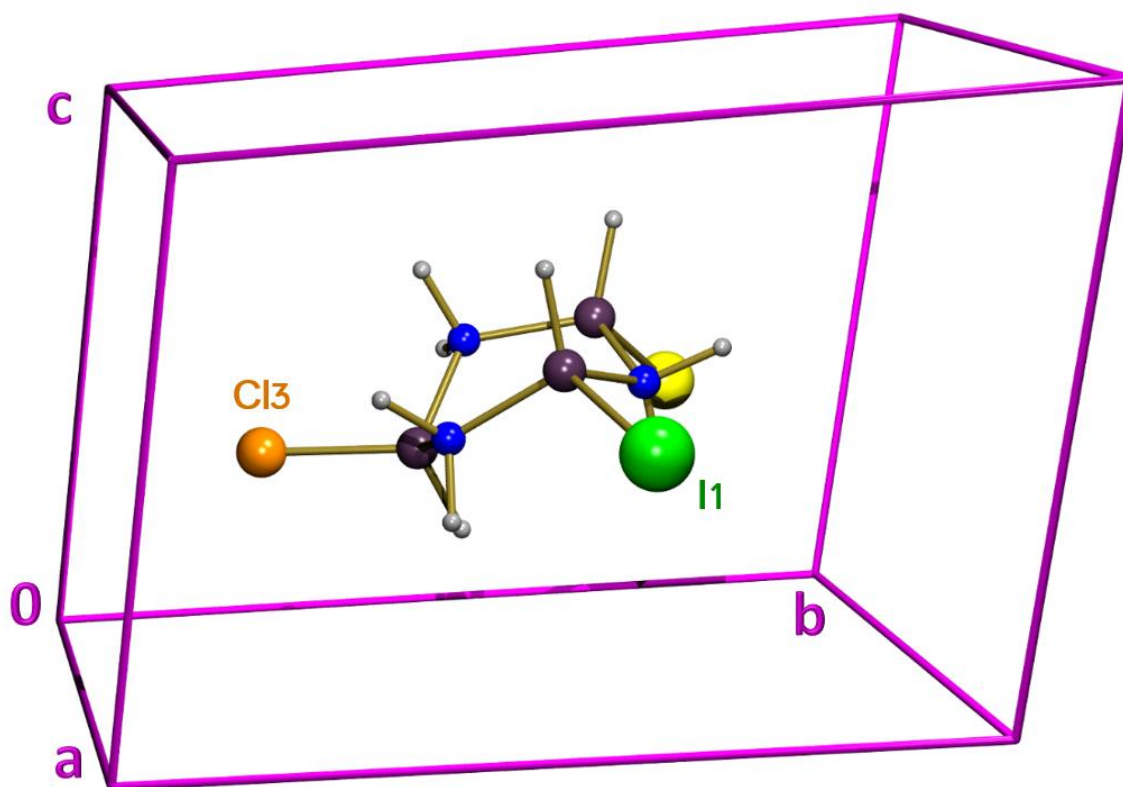


**Figure 16.** Location of the ( $B_3N_3H_9IBrCl$ ) molecule in the simulated unit cell.

The format of the input file is as follows:

```
proj2, half sphere, sin(theta)/lambda max = 0.70 angstroms^-1
CELL 10.158512 10.253285 7.476376 74.5772 75.7351 68.1241
      H      K      L      F      REAL PART  IMAG. PART
1      0      0      26.500000    -0.1866E+02  -0.1882E+02
2      0      0      33.060000    -0.3228E+02  -0.7139E+01
3      0      0      65.580000    -0.6557E+02  -0.1282E+01
4      0      0      16.940000    -0.1335E+01   0.1689E+02
5      0      0      33.560000     0.3356E+02   0.3046E+00
. . . . .
. . . . .
7      6     10      5.040000     0.3573E+01  -0.3555E+01
3      7     10      5.420000     0.4992E+01   0.2111E+01
4      7     10      4.730000     0.4653E+01  -0.8514E+00
5      7     10      1.000000    -0.7529E+00  -0.6582E+00
6      7     10      4.310000    -0.3993E+01  -0.1622E+01
```

**Line 1:** This is a comment line, one can put whatever s(he) wants there, but you need to read this comment and print it out before doing anything else

**Line 2:** The keyword "CELL" is followed by six unit cell parameters:  $a$ ,  $b$ ,  $c$  (all in angstroms, Å), and  $\alpha$ ,  $\beta$ ,  $\gamma$  (all in degrees, °).

**Line 3:** This is just a header for the  $hkl$  data.

**Lines 4...:** These are the actual data lines. The first three numbers in each line give the  $h$ ,  $k$ , and  $l$  values for each reflection ( $hkl$ ). The remaining numbers are  $|F(hkl)|$ ,  $A(hkl)$  and  $B(hkl)$ . It can be verified that for each reflection,

$$|F(hkl)| = \sqrt{A(hkl)^2 + B(hkl)^2} \quad (49)$$

The number of data lines can vary from 100 to, say,  $10^6$ , but you never know in advance how many data points there are in a given file. **Note that only half of the data set is given in the input file (Friedel's law), so after summing up you should multiply the sum by 2.**

## 6. Suggested Implementation and the Code Requirements

1. Read in the unit cell parameters and the  $hkl$  data
2. Calculate the volume of the unit cell. It can be done either using equation (1) or via the *metric tensor*  $\mathbf{G}$

$$\mathbf{G} = \begin{pmatrix} \mathbf{a} \cdot \mathbf{a} & \mathbf{a} \cdot \mathbf{b} & \mathbf{a} \cdot \mathbf{c} \\ \mathbf{b} \cdot \mathbf{a} & \mathbf{b} \cdot \mathbf{b} & \mathbf{b} \cdot \mathbf{c} \\ \mathbf{c} \cdot \mathbf{a} & \mathbf{c} \cdot \mathbf{b} & \mathbf{c} \cdot \mathbf{c} \end{pmatrix} \quad (50)$$

where the symbol ' $\cdot$ ' indicates the scalar (dot) product of two vectors. The determinant of the metric tensor  $\mathbf{G}$  is equal to the square of the volume of the unit cell:

$$V_c = [\det(\mathbf{G})]^{1/2} \quad (51)$$

3. Compute the orthonormalization matrix  $\mathbf{M}$  that converts a point with fractional coordinates  $\mathbf{x}_f$  to the Cartesian system ( $\mathbf{x}_c$ ) (see Figure 17):

$$\mathbf{x}_c = \mathbf{M} \mathbf{x}_f \quad (52)$$

Of course, the inverse of matrix  $\mathbf{M}$  does the opposite:

$$\mathbf{x}_f = \mathbf{M}^{-1} \mathbf{x}_c \quad (53)$$

Note that  $\mathbf{G} = \mathbf{M}^T \mathbf{M}$ . There are infinite number of ways to transform a crystallographic frame to a Cartesian frame. I suggest the following form of matrix  $\mathbf{M}$ :

$$\mathbf{M} = \begin{pmatrix} a & b \cos \gamma & c \cos \beta \\ 0 & b \sin \gamma & c(\cos \alpha - \cos \beta \cos \gamma) / \sin \gamma \\ 0 & 0 & c[\sin^2 \gamma - (\cos^2 \alpha + \cos^2 \beta - 2 \cos \alpha \cos \beta \cos \gamma)]^{1/2} / \sin \gamma \end{pmatrix} \quad (54)$$

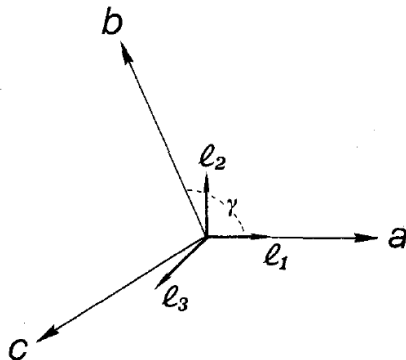


**Figure 17.** Orthonormalization of crystallographic bases. [2]

4. In order to search for atoms, i.e. peaks of the electron density distribution function,  $\rho(xyz)$ , it is convenient to define a starting set of grid points in the crystallographic frame, but to perform the actual search in the Cartesian frame.

One of course, can search the entire unit cell, but in order to speed up the process I recommend the following grid search limits [*for this particular problem only!*] defined in the crystallographic frame (i.e. fractional coordinates)

$$\begin{aligned} 0.1 &\leq x_f \leq 0.9 \\ 0.1 &\leq y_f \leq 0.9 \\ 0.1 &\leq z_f \leq 0.9 \end{aligned} \quad (55)$$

The spacing between the grid points should not be too large, perhaps not more than 0.4 angstroms.

5. For a peak search you need to use **a)** the Newton-Raphson (NR) optimization algorithm [7] and **b)** its modification known as the eigenvector following (EF) method [8,9,10]. In the following, I use references [8] and [10] to describe the two methods *in the Cartesian frame*.

The NR algorithm departs from a truncated Taylor expansion at a point  $\mathbf{x} = \mathbf{x}_0 + \mathbf{h}$ , where

$$\mathbf{x} \equiv \begin{pmatrix} x \\ y \\ z \end{pmatrix}, \quad \mathbf{x}_0 \equiv \begin{pmatrix} x_0 \\ y_0 \\ z_0 \end{pmatrix}, \quad \mathbf{h} \equiv \begin{pmatrix} h_x \\ h_y \\ h_z \end{pmatrix}, \quad (56)$$

about  $\mathbf{x}_0$  of a multidimensional twice-differentiable function scalar function [8,10],

$$\rho(\mathbf{x}) = \rho(\mathbf{x}_0) + \mathbf{g}_0^T \mathbf{h} + \frac{1}{2} \mathbf{h}^T \mathbf{H}_0 \mathbf{h} + \dots \quad (57)$$

where  $\rho(\mathbf{x})$  is the electron density,  $\mathbf{g}_0$  and  $\mathbf{H}_0$  are the *gradient vector* and *Hessian matrix* of  $\rho$  at point  $\mathbf{x}_0$  respectively:

$$\mathbf{g}_0 = \nabla \rho(\mathbf{x}_0) \equiv \begin{pmatrix} \frac{\partial \rho(\mathbf{x}_0)}{\partial x} \\ \frac{\partial \rho(\mathbf{x}_0)}{\partial y} \\ \frac{\partial \rho(\mathbf{x}_0)}{\partial z} \end{pmatrix} \quad (58)$$

$$\mathbf{H}_0 = \nabla^2 \rho(\mathbf{x}_0) \equiv \begin{pmatrix} \frac{\partial^2 \rho(\mathbf{x}_0)}{\partial x \partial x} & \frac{\partial^2 \rho(\mathbf{x}_0)}{\partial x \partial y} & \frac{\partial^2 \rho(\mathbf{x}_0)}{\partial x \partial z} \\ \frac{\partial^2 \rho(\mathbf{x}_0)}{\partial y \partial x} & \frac{\partial^2 \rho(\mathbf{x}_0)}{\partial y \partial y} & \frac{\partial^2 \rho(\mathbf{x}_0)}{\partial y \partial z} \\ \frac{\partial^2 \rho(\mathbf{x}_0)}{\partial z \partial x} & \frac{\partial^2 \rho(\mathbf{x}_0)}{\partial z \partial y} & \frac{\partial^2 \rho(\mathbf{x}_0)}{\partial z \partial z} \end{pmatrix} \quad (59)$$



Truncating this expansion at the quadratic term and applying the stationary condition

$$\frac{\partial \rho(\mathbf{x}_0)}{\partial \mathbf{h}} = 0 \quad (60)$$

leads to the prediction that the best step  $\mathbf{h}$  (NR step) to get from the current point  $\mathbf{x}_0$  to the desired maximum at  $\mathbf{x}$  is then simply [8,10]

$$\mathbf{h} = -\mathbf{H}_0^{-1} \mathbf{g}_0 \quad (61)$$

The geometric interpretation of the NR method is that at each iteration one approximates  $\rho(\mathbf{x})$  by a quadratic function around  $\mathbf{x}_0$ , and then takes a step towards the stationary point (in several dimensions it can be either a maximum, a minimum, or a saddle point) [11]. Note that if  $\rho(\mathbf{x})$  happens to be a quadratic function, then the exact extremum is found in one step [11].

An equivalent expression for equation (61) in terms of the eigenvectors  $\mathbf{v}_i$ , and eigenvalues  $b_i$ , of the Hessian  $\mathbf{H}_0$  is given by [8,10]

$$\mathbf{h} = -\sum_{i=1}^3 \frac{F_i \mathbf{v}_i}{b_i} \quad (62)$$

where  $F_i = \mathbf{v}_i^T \mathbf{g}_0$  is the projection of the gradient  $\mathbf{g}_0$  along the local eigenmode  $\mathbf{v}_i$ . The Hessian eigenvalues  $b_i$  (and the corresponding eigenvectors  $\mathbf{v}_i$ ) are assumed to be ordered as  $b_1 < b_2 < b_3$  [8], though at this stage the order is irrelevant. In the present notation, the  $i$ -th eigenvector  $\mathbf{v}_i$  is a *column* vector defined as

$$\mathbf{v}_i \equiv \begin{pmatrix} v_{i,x} \\ v_{i,y} \\ v_{i,z} \end{pmatrix} \quad (63)$$

Note that equation (62) can be written out explicitly as

$$\mathbf{h} = -\left[ \left( \frac{F_1}{b_1} \right) \mathbf{v}_1 + \left( \frac{F_2}{b_2} \right) \mathbf{v}_2 + \left( \frac{F_3}{b_3} \right) \mathbf{v}_3 \right] \quad (64)$$

An important insight [12] in the essence of the behavior of NR can be gained from this equation: NR *minimizes* along modes with *positive* Hessian eigenvalue and vice versa [8]. Let us assume for a moment that we want to locate a saddle point on an energy surface starting in a region where the Hessian has one negative eigenvalue. In that region the NR step is appropriate because it does exactly what is required: maximizing along one mode while minimizing along the others. Thus the aforementioned insight can be generalized as follows: *NR is only suitable for the location of a critical point provided one is already in a region where the Hessian has the correct structure* [8].

The EF method however offers a way to leave a wrong region for one where the Hessian has the correct structure by modifying equation (62) [8, 9,10,12],

$$\mathbf{h} = -\sum_{i=1}^3 \frac{F_i \mathbf{v}_i}{b_i - \lambda_{\text{EF}}} \quad (65)$$

where the 'shift' parameter  $\lambda_{\text{EF}}$  needs to be determined. A deeper analysis by Banerjee et al. [13] proposes that the shift parameter  $\lambda_{\text{EF}}$  for the case in which  $\rho(\mathbf{x})$  is maximized is obtained from the solutions of the following eigenvalue equation [8,10]:

$$\mathbf{B}' \mathbf{h}' = \lambda \mathbf{h}' \quad (66)$$

$$\begin{pmatrix} b_1 & 0 & 0 & F_1 \\ 0 & b_2 & 0 & F_2 \\ 0 & 0 & b_3 & F_3 \\ F_1 & F_2 & F_3 & 0 \end{pmatrix} \begin{pmatrix} h_x \\ h_y \\ h_z \\ 1 \end{pmatrix} = \lambda \begin{pmatrix} h_x \\ h_y \\ h_z \\ 1 \end{pmatrix} \quad (67)$$

where  $\lambda_{\text{EF}}$  is the *highest* eigenvalue of the respected set of solutions  $\lambda_i$  ( $i=1,4$ ). Note that if you wish to find a minimum or a saddle point of a function, the procedure is very similar - see reference [8].

In summary, the sequence of operations for a  $k$ -th EF step at  $\mathbf{x}_k$  is as follows:

- a) calculate  $\rho(\mathbf{x}_k)$ ,  $\mathbf{g}_k$ , and  $\mathbf{H}_k$
- b) diagonalize  $\mathbf{H}_k$  to get its three eigenvalues ( $b_i, i=1,3$ ) and eigenvectors ( $\mathbf{v}_i, i=1,3$ )
- c) calculate  $F_i = \mathbf{v}_i^T \mathbf{g}_k$  ( $i=1,3$ )
- d) construct matrix  $\mathbf{B}'$  as shown in equation (67)
- e) diagonalize matrix  $\mathbf{B}'$  to obtain the set of four eigenvalues  $\lambda_i$  ( $i=1,4$ )
- f) determine  $\lambda_{\text{EF}}$  which is the *highest* eigenvalue of the set of solutions  $\lambda_i$  ( $i=1,4$ )
- g) recalculate vector  $\mathbf{h}$  using equation (65) and  $\lambda_{\text{EF}}$  obtained in the previous step
- h) advance from  $\mathbf{x}_k$  to  $\mathbf{x}_{k+1}$ :  $\mathbf{x}_{k+1} = \mathbf{x}_k + \mathbf{h}$

Keep in mind that you may still want to set up a certain limit for the size of each EF step, for example 0.25 Å seems to be a good choice [*for this particular problem!*], and the maximum number of EF steps taken from a given starting point (for example, no more than 15-20).

The stopping criterion should be related to the norm of the gradient vector of  $\rho$ , for example, a reasonable value can be around  $10^{-5}$ - $10^{-7}$  electrons Å<sup>-4</sup>.

It may also be a good idea to check the curvature for any found point with the gradient norm below abovementioned criterion. It is important to verify that the found point is indeed a maximum in  $\rho$ . The best way to identify a maximum is to check signs of the three Hessian eigenvalues - for a maximum, all three should be negative.

Also note that because of a limited number of terms in the Fourier series expansion, the landscape of  $\rho$  will be very noisy - there are going to be many “false” maxima. Perhaps, the best way to separate those is to check the value of  $\rho$  at each found maximum. For this particular dataset, the non-hydrogen atoms correspond to the peaks with the “height” of above 8 electrons Å<sup>-3</sup>, while for hydrogen atoms the peaks should be around 2.5-3.5 electrons Å<sup>-3</sup>.

Keep in mind that you may be able to reach the same maximum from different starting points, therefore the program should always check whether the found maximum is already present in the list. *Duplicate entries need to be discarded from the final peak list.*

6. The density at each point with fractional coordinates  $\mathbf{x}_f$  is given by

$$\rho(\mathbf{x}_f) = \frac{1}{V_c} \sum_{h=h_{\min}}^{h_{\max}} \sum_{k=k_{\min}}^{k_{\max}} \sum_{l=l_{\min}}^{l_{\max}} \{A(hkl) \cos[2\pi(hx_f + ky_f + lz_f)] + B(hkl) \sin[2\pi(hx_f + ky_f + lz_f)]\} \quad (68)$$

However, it may be desirable to calculate the derivatives of  $\rho$  in the Cartesian frame. The relationship between the Cartesian  $\mathbf{x}_c$  and fractional (crystallographic)  $\mathbf{x}_f$  coordinates is given above - see equations (52) and (53).

Also, keep in mind that because only half of the necessary reflections are present in the input file (Friedel's law), equation (68) (and the derivatives) should include a factor of 2.

7. This problem is ideally suited for exploring parallelism because the calculation of contribution of a given  $(hkl)$  to  $\rho$  and its derivatives at a given point does not depend on other entries. Therefore, it is advisable (*but not required!*) to parallelize the calculation of  $\rho$  and its derivatives at a given point by splitting the job over multiple cores (processors). It should be relatively easy to implement in Mathematica, Matlab, and Maple.
8. To help you debug your code, an ASCII file with the list of fractional coordinates of atoms in the structure has been uploaded to D2L. For your convenience, it is also given below:

	$x_f$	$y_f$	$z_f$
I1	0.816559	0.605285	0.443681
Br2	0.184553	0.732849	0.422528
Cl3	0.538601	0.187547	0.425822
N4	0.483883	0.646545	0.488147
N5	0.378678	0.442024	0.561205
N6	0.649648	0.394286	0.452607
B7	0.343047	0.604230	0.576299
B8	0.623600	0.524422	0.547738
B9	0.510127	0.380557	0.407817
H10	0.701261	0.302105	0.537015
H11	0.719691	0.398985	0.328848
H12	0.487896	0.449970	0.255478
H13	0.472473	0.735457	0.535232
H14	0.492243	0.677623	0.345111
H15	0.609035	0.488668	0.714905
H16	0.306873	0.618111	0.736486
H17	0.290188	0.433251	0.530414
H18	0.391646	0.378086	0.690668

Since you know the location of each atom, *at the very end of the run your code should print out a table in which atoms given in the list above are “matched” against the found peaks.* For each atom, a distance (in Å) to the closest peak (and, of course, the peak number) should be printed out. A successful match, when the distance between an atom and a found peak is below 0.1 Å, should be identified with an asterisk (\*). In addition, print out the value of  $\rho$  (in  $\text{e} \text{Å}^{-3}$ ) at the found peak in the same line as shown in the table below:

Atoms and closest peaks:

#	Atom	-----	xyz (FRA)	-----	-----	dist to	closest peak	-----
1	I1	0.81656	0.60528	0.44368	*	0.0000A	from peak 18, rho =	124.324 e/A^3
2	Br2	0.18455	0.73285	0.42253	*	0.0012A	from peak 1, rho =	80.628 e/A^3
3	Cl3	0.53860	0.18755	0.42582	*	0.0026A	from peak 12, rho =	33.860 e/A^3
4	N4	0.48388	0.64655	0.48815	*	0.0041A	from peak 11, rho =	10.151 e/A^3
5	N5	0.37868	0.44202	0.56120	*	0.0146A	from peak 6, rho =	10.056 e/A^3
6	N6	0.64965	0.39429	0.45261	*	0.0048A	from peak 15, rho =	10.291 e/A^3
7	B7	0.34305	0.60423	0.57630	*	0.0210A	from peak 4, rho =	6.903 e/A^3
8	B8	0.62360	0.52442	0.54774	*	0.0385A	from peak 14, rho =	6.847 e/A^3
9	B9	0.51013	0.38056	0.40782	*	0.0103A	from peak 9, rho =	7.158 e/A^3
10	H10	0.70126	0.30211	0.53702	*	0.0288A	from peak 16, rho =	2.807 e/A^3
11	H11	0.71969	0.39898	0.32885	*	0.0740A	from peak 17, rho =	2.908 e/A^3
12	H12	0.48790	0.44997	0.25548	*	0.0229A	from peak 10, rho =	2.801 e/A^3
13	H13	0.47247	0.73546	0.53523	*	0.0330A	from peak 8, rho =	3.235 e/A^3
14	H14	0.49224	0.67762	0.34511	*	0.0548A	from peak 7, rho =	3.053 e/A^3
15	H15	0.60903	0.48867	0.71491	*	0.0275A	from peak 13, rho =	2.747 e/A^3
16	H16	0.30687	0.61811	0.73649	*	0.0529A	from peak 3, rho =	2.834 e/A^3
17	H17	0.29019	0.43325	0.53041	*	0.0705A	from peak 2, rho =	2.858 e/A^3
18	H18	0.39165	0.37809	0.69067	*	0.0155A	from peak 5, rho =	2.883 e/A^3

*While you do not have to use exactly the same format, you absolutely need to print out a table that contains all the required information.*

Note how the “height” of the electron density peak correlates with the number of electrons in an atom: the largest peak of  $\sim 124 \text{ e } \text{\AA}^{-3}$  corresponds to the iodine atom (53 electrons), the second largest peak of  $\sim 81 \text{ e } \text{\AA}^{-3}$  belongs to the bromine atom (35 electrons), etc. all the way down to the smallest peaks of  $\sim 3 \text{ e } \text{\AA}^{-3}$  that identify the hydrogen atoms (1 electron in each atom). *Note: when generating the structure factor data, the instructor had to increase the number of electrons in each hydrogen atom in order to make them clearly “visible” in the Fourier space.*

9. Finally, the runtime of the program should be under 1 hour for the provided dataset.

**That's it! Do not forget to submit your program to D2L by the due date/time.**

## References

- [1] Atkins, P; de Paula, J. *Physical Chemistry*, 8th edition, W. H. Freeman and Company, New York, 2006.
- [2] Giacovazzo, C., Monaco, H. L., Artioli, G., Viterbo, D., Milaneso, M., Ferraris, G., Gilli, G., Gilli, P., Zanotti, G., Catti, M. *Fundamentals of Crystallography*, 3rd edition, Oxford University Press, 2011.
- [3] Fletcher, R. *Practical Methods of Optimization*, 2nd edition, John Wiley & Sons, 1987.
- [4] Bokii, G. B., Parai-Koshits, M. A., *Rentgenostrukturnyi analiz (X-ray Structure Analysis)* [in Russian], Izd. Mosk. Gos. Univ., Moscow, 1964.
- [5] Ladd, M. F. C., Palmer, R. A. *Structure Determination by X-ray Crystallography*, 4th edition, Springer, 2003.
- [6] Schwarzenbach, D. *Crystallography*, Wiley, 1997.
- [7] Press, W. H., Teukolsky, S. A., Vetterling, W. T., Flannery, B. P. *Numerical Recipes 3rd Edition: The Art of Scientific Computing*, 3rd edition. Cambridge University Press, 2007.
- [8] Popelier P. *A robust algorithm to locate automatically all types of critical-points in the charge-density and its Laplacian*. Chemical Physics Letters. 228, 160-164, 1994.
- [9] Cerjan, C. J., Miller, W. H. "On finding transition states", J. Chem. Phys. 75, 2800, 1981.
- [10] Baker, J. *An algorithm for the location of transition states*. Journal of Computational Chemistry, 7, 385-395, 1986.
- [11] [http://en.wikipedia.org/wiki/Newton%27s\\_method\\_in\\_optimization](http://en.wikipedia.org/wiki/Newton%27s_method_in_optimization)
- [12] J. Simons, P. Jorgensen, H. Taylor and J. Ozment, *Walking on Potential Energy Surfaces*. J. Phys. Chem. 87 (1983) 2745.
- [13] A. Banerjee, N. Adams, J. Simons and R. Shepard, *Search for Stationary Points on Surfaces*. J. Phys. Chem. 89 (1985) 52.